

Technosols constructed from urban waste enhance carbon stabilization through improved soil aggregation

Thalita Fernanda Abbruzzini^{1*}, Blanca Lucia Prado Pano¹, Lucy Mora Palomino¹, Alan Ulises Loredó-Jasso¹, María del Pilar Ortega Larrocea¹, Ceres Perez Vargas², Victor Manuel Peña Ramirez³

¹ Instituto de Geología, Departamento de Ciencias Ambientales y del Suelo, Universidad Nacional Autónoma de México, México

² Posgrado en Ciencias de la Tierra, Universidad Nacional Autónoma de México, México

³ Universidad Autónoma Metropolitana Iztapalapa, México

Corresponding author: E.mail: thalita@geologia.unam.mx

Article info

Received 22/1/2025; received in revised form 28/1/2025; accepted 3/2/2025

DOI: [10.6092/issn.2281-4485/21163](https://doi.org/10.6092/issn.2281-4485/21163)

© 2025 The Authors.

Abstract

This study investigates the distribution and stabilization of carbon (C) in technosols constructed from urban waste materials and organic inputs, aiming to enhance C storage and restore urban ecosystems. Technosols composed of concrete (*Cw*) and excavation (*Ev*) waste, wood chips (*W*), compost (*C*), and biochar (*B*) (*CwO*, *EvO*, and *WCB*) were analyzed over two years within an urban milpa, a traditional Mesoamerican agricultural system. We assessed C and nitrogen (N) contents, exchangeable cations, aggregate size distribution, and molecular composition. Among the technosols, the wood chip, compost, and biochar mixture (*WCB*) exhibited the highest organic C (OC), inorganic C (IC), and total N (TN) contents, followed by *CwO* and *EvO*. While C levels remained stable in all technosols, TN decreased in *CwO*, increasing its C/N ratio to 27, indicating potential N immobilization. Calcium concentrations increased across all technosols (*CwO* = *WCB* > *EvO*), while Na levels decreased, improving aggregate stability. Macroaggregates accounted for 85% of OC and TN in all technosols, with microaggregates and silt + clay fractions containing 5% and 10%, respectively. *CwO* and *EvO* exhibited particulate organic matter occlusion within macroaggregates, while *EvO* had more microaggregates and silt + clay particles. FTIR analysis confirmed the presence of carbonates in all aggregate sizes and showed that the molecular composition of stabilized C varied, with more recalcitrant compounds found in microaggregates. These results highlight the importance of managing cation balances, particularly increasing Ca^{2+} and reducing Na^+ , to improve soil structure and enhance C stabilization.

Keywords: Carbon storage, Concrete waste, Excavation waste, FTIR spectroscopy, Urban farming, Urban soils

Introduction

The global population is increasingly urban with 57% living in urban areas. By 2050, the world population will increase by more than 2 billion people mostly in urban areas of developing countries (UN-Habitat Core Team 2022). Mexico City, one of the largest and

most populous cities in the world, has experienced rapid urbanization, expanding largely on fertile agricultural land (Cruz-Bello et al. 2023; Lima et al. 2023). Currently, 47% of its territory is sealed by impervious surfaces, while unsealed soils suffer from compaction, contamination, and pollution, limiting

ecosystem services like plant growth and carbon storage (O’Riordan et al. 2021). The city generates 13,000 tons of solid urban waste (SUW) daily, 57% of which is poorly managed, exacerbating soil degradation (SEDEMA 2021; PAOT-EOT-02–2010, 2011). To promote sustainable urban development, planters can reintroduce green spaces in cities for food and non-food production, while also restoring soil functions in contaminated or degraded sites. However, these practices often require large amounts of soil, typically sourced from pristine periurban areas, which can degrade natural buffer zones and protected areas (Séré et al. 2008; Rokia et al. 2014; Prado et al. 2020; Abbruzzini et al. 2022). To address this, researchers have proposed technosols, constructed soils that mimic natural soil functions and mitigate urban environmental impacts through resource efficiency (Deeb et al. 2016). Composed of waste, by-products, and organic or inorganic raw materials, technosols offer ecosystem services such as improved air quality, pollution mitigation, enhanced water runoff and quality, biomass production, biodiversity maintenance, local climate regulation, carbon storage, and the protection of natural soil resources (Morel et al. 2015; Deeb et al. 2016; Grard et al. 2018). Despite the fact that formation and pedogenesis of constructed technosols appear to be similar to those happening in natural soils in the short-term (< 3 years) (Séré et al. 2010, Frouz et al. 2013, Jangorzo et al. 2015, Leguédou et al. 2016, Vergnes et al. 2017), it is difficult to predict aggregation and formation of organomineral associations when mixing technogenic materials together, and it is even harder to determine the stability of these associations in the created substrates (Vidal-Beaudet et al. 2018). Technogenic parent materials may undergo accelerated physical and chemical changes during the early evolution of constructed soils (Séré et al. 2010). This occurs because the formation, functioning, and pedogenic evolution of young technosols are strongly influenced by the diverse origin and unusual chemical composition of the technogenic parent materials (Séré et al. 2010, Moreno-Barriga et al. 2017, Vidal-Beaudet et al. 2018) that likely differ from natural soils regarding the way they are prepared and assembled (e.g., crushing, sieving, drying, mixing), as well as their management and various disturbances they can undergo over time (e.g., organic amendments, plant growth, microbial and faunal activities, tillage, compaction, pollution, mineral fertilization) (Deeb et al. 2016). Notably, there have been significant changes

in the spatial arrangement of particles, such as sand, silt, clay, and organic matter (OM) in technosols. These particles aggregate and stabilize through various physico-chemical and biological interactions at different scales, forming distinct structural units known as aggregates (Deeb et al. 2017; Moreno-Barriga et al. 2017; Séré et al. 2010; Ruiz et al. 2020). Urban wastes from construction, excavation, and demolition contain a mix of inorganic and organic materials with varied composition and particle size, contributing to the formation of soil aggregates and protecting organic carbon (Lorenz and Kandeler 2006; Prado et al. 2020; Tisdall and Oades 1982). Organic amendments like compost, wood chips, and biochar introduce macromolecules (e.g., lignin, cellulose) that enhance the longevity and chemical stability of organic matter (Hernandez-Soriano et al. 2016; Forján et al. 2018; Rakhsh et al. 2017; Abbruzzini et al. 2022) through recalcitrance, microbial processes, and organomineral interactions (Liang et al. 2017). Studies show technosols with well-mixed parent materials can sustain high organic carbon levels over time (Rees et al. 2019; Ivashchenko et al. 2021). However, the dynamics of organic C pools and their interactions with minerals in technosols remain underexplored (Vidal-Beaudet et al. 2018; Rees et al. 2019), with few urban field trials addressing these processes (Boneta et al. 2019; Deeb et al. 2020). This study provides a quantitative and qualitative assessment of technosols and their aggregate size classes two years after the establishment of an urban milpa, a traditional intercropping system with maize, beans, squash, and other species. The technosols were constructed using excavation and concrete waste as inorganic parent materials, combined with wood chips, compost, and biochar as organic amendments. We hypothesized that: i) raw material type and experimental period significantly impact the physicochemical, chemical, and biological properties of technosols; ii) excavation waste contributes more cementing agents than concrete waste for aggregate formation; iii) larger aggregates accumulate more organic carbon (OC) than smaller ones, irrespective of technosol type; and iv) organic and mineral functional compounds associate differently across aggregate size classes depending on the materials used. The study aims to enhance understanding of pedogenic processes and C stabilization in technosols constructed from urban waste, offering a strategy to improve ecosystem services in cities.

Materials and methods

Collection and composition of raw materials

The raw materials used in this study were concrete waste (*Cw*), excavation waste (*EW*), wood chips (*W*), compost (*C*), and biochar (*B*). *Cw* and *EW* were sourced from a private company in Mexico City (Concretos Recicladados S.A. de C.V.), which recycles construction waste. *Cw* is a mix of ground concrete, bricks, masonry, and ceramics, with an average grain

size of 6.35 mm. *EW* is a soil-like material, sieved (< 4 mm) to remove larger debris. *W* was sourced from the Composting Plant of the National Autonomous University of Mexico (UNAM), while *C* came from the Iztapalapa Composting Plant. *B* was produced from wood chips, sun-dried, and pyrolyzed in a Kon-Tiki kiln (Schmidt and Taylor 2014). The organic raw materials differed significantly from each other and from the inorganic materials, regarding their physicochemical and chemical properties (Table 1).

Table 1. Basic characterization of the raw materials used for the construction of technosols. Values represent the mean ($n=2$). Means followed by the same uppercase letters do not differ statistically among themselves by Tukey's test at 5% probability. (^aPrado et al. 2020; ^bAbbruzzini et al. 2021)

Parent materials	pH (H ₂ O)	Electrical conductivity (EC)	Total C	Total N	C/N	Texture		
		μS cm ⁻¹	g kg ⁻¹			Sand	Silt	Clay
						%		
Concrete waste ^{a,b}	8.1	1970	21.9	0.8	49.1	64.3	32.1	3.6
Excavation waste ^{a,b}	7.7	295	9.1	0.5	12.1	75.2	23.0	1.8
Wood chips ^b	5.3	584	451	8.1	55.7	-	-	-
Compost ^b	7.0	5860	200	19.8	10.1	-	-	-
Biochar ^b	7.9	1354	740	7.0	106.4	-	-	-

Experimental setup and analysis of technosols

Three technosols were evaluated: *CwO* (30% *Cw*, 25% *W*, 25% *C*, 20% *B*), *EW*O (30% *EW*, 25% *W*, 25% *C*, 20% *B*), and *WCB* (55% *W*, 25% *C*, 20% *B*). Plots were installed in UNAM's campus, arranged in a complete block design with three plots per technosol (9 plots total, $n = 3$ per technosol), each measuring 1.45 x 1.40 m with a depth of 0.4 m. Maize and beans were grown during the rainy season for two years, with no mineral fertilizer applied. Samples were taken from the surface layer (0-0.2 m depth) before each growing season. Maize had biomass growth (Table 2), but its grain harvest was limited mainly by the presence of squirrels in the experimental site, so yields were only estimated for beans. The technosols were analyzed for organic (OC) and inorganic carbon (IC), total nitrogen (TN), exchangeable cations (Ca²⁺, Mg²⁺, K⁺, Na⁺), and texture (sand, silt, clay proportions). Surface samples (0-0.2 m depth) were collected before each growing season (initial conditions, 1 year, and 2 years). OC, IC, and TN contents were determined by total combustion (Perkin Elmer 2400 series II), with OC measured after hydrochloric

acid (HCl 0.5 N) treatment and IC calculated as the difference between total and OC contents. Exchangeable cations were extracted with ammonium at pH 7 and measured by Atomic Absorption Spectrometry (Perkin Elmer Pin AAcle 900), while texture was analyzed using the sieve-pipette method (Gee and Or, 2002).

Table 2. Dry biomass (above and below ground) of maize and beans, and grain yield of beans in Technosols. Mean values followed by the same letter do not differ statistically from each other according to Tukey's test at 5 % probability level.

Technosol	Dry biomass (above and below ground)		Grain yield
	Maize (g)	Beans (g)	
<i>CwO</i>	296.4 (51.6) A	39.2 (2.08) A	57.4 (3.84) A
<i>EW</i> O	416.2 (75.7) A	31.1 (1.85) A	41.2 (4.02) B
<i>WCB</i>	259.8 (59.4) A	34.5 (2.00) A	47.6 (4.08) AB

Micromorphological analysis of whole soil samples

Thin sections were prepared from undisturbed samples (5 cm diameter, 5 cm height) collected 2 years after plot installation. Samples were dried at 60 °C, then impregnated with polyester resin mixed with styrene monomer, methyl ethyl ketone peroxide, and a K-2000 catalyst, followed by vacuum treatment at 22 atm for 30 minutes. After air drying, the hardened blocks were segmented with a diamond blade cutter, polished with sandpaper (120-600 grit), and resin-bonded to petrographic slides. The sections were thinned to 30 microns using tungsten carbide abrasives. Thin sections were examined with an Olympus BX51 microscope using normal and crossed Nicols light to observe mineral birefringence, mineral weathering, organic material degradation, aggregate formation, and faunal activity.

Aggregate size distribution and stability in technosols

Samples of each technosol were passed through an 8 mm sieve to remove stones and coarse roots, and aggregate size distribution was determined using wet sieving (Díaz-Zorita et al. 2002; Almajmaie et al. 2017). A 20 g soil sample was placed on a stack of sieves with mesh sizes of 2 mm, 1 mm, 0.5 mm, 0.25 mm, and 0.053 mm. The sieves were submerged in water and shaken for 5 minutes at 23 cycles per minute with a 3 cm stroke amplitude. Water-stable aggregates were recovered, dried at 105 °C, and weighed. The size classes obtained were: (i) > 2 mm (large macroaggregates); (ii) 2–0.25 mm (small macroaggregates); (iii) 0.25–0.053 mm (microaggregates); and (iv) < 0.053 mm (silt + clay). For the smallest size class, 10 mM CaCl₂ was added to the water-soil suspension. Samples were homogenized, dried at 60 °C, and weighed for dry matter determination. OC, IC, and TN contents in each size class were determined by total combustion (Nelson and Sommers 1996) using a CNHS/O elemental analyzer (Perkin Elmer 2400 series II). Soil aggregation was evaluated using the mean weight diameter (MWD) to assess size distribution and the mean geometric diameter (MGD) to identify predominant size classes. The values of MWD [Eq. 1] (Kemper and Rosenau 1986) and MGD [Eq. 2] (Mazurak 1950) were determined as follows:

$$DMP(mm) = \sum_{i=1}^n x_i w_i \quad [1]$$

$$DMG(mm) = \exp \left[\frac{\sum_{i=1}^n w_i \log x_i}{\sum_{i=1}^n w_i} \right] \quad [2]$$

where: w_i is the proportion of each aggregate size class in relation to the total amount, and x_i is the mean diameter of the size classes (mm).

Infrared spectroscopic characterization of aggregate size classes

Fourier transform infrared spectroscopy (FTIR) was used to characterize organic and mineral components at the molecular level, inferring chemical reactivity and interactions with the mineral phase that form stable aggregates (Ellerbrock and Gerke 2013). Specific absorption bands indicated functional groups, serving as a fingerprint of soil organic matter composition (Raphael 2011). FTIR was performed in triplicate ($n = 3$) for each aggregate size class using Diffuse Reflectance (DRIFT) on a Varian 3100 Excalibur Spectrometer with an EasiDiff accessory. A 0.3 mg sample was combined with 99.7 mg of KBr, dried in a desiccator, and analyzed in the mid-FTIR range (4000–400 cm⁻¹) with 4 cm⁻¹ resolution and 64 scans per sample. Spectra were averaged for each aggregate size class, with baseline shifts corrected via Iterative Restricted Least Square (IRLS) and spectra smoothed using a moving average filter (11 bands) with the 'baseline' and 'prospectr' R packages (Liland et al. 2010; Stevens and Ramirez-Lopez 2020).

Statistical analysis

A linear model was applied to analyze the contents of C, N, and exchangeable cations in technosols, aggregate size class distribution, MWD, MGD, and C and N contents in aggregates. A generalized linear model (GLM) with a binomial distribution was used to examine mycorrhizal root colonization. All parameters were analyzed with ANOVA, and post-hoc Tukey's test was applied at a 5% significance level. Principal component analysis and Pearson correlation coefficients explored relationships between physicochemical properties and the molecular composition of organic and inorganic compounds in different aggregate size classes. Statistical analyses were performed using R software (R Core Team 2022).

Results and discussion

Carbon and nitrogen dynamics in technosols

Organic carbon (OC) contents varied significantly among the three technosols ($p = 6.85e-12$) and over

time ($p = 8.74e-06$). The wood chip, compost, and biochar (*WCB*) technosol had the highest OC content (277 g kg^{-1}), followed by concrete waste (*CwO*, 193 g kg^{-1}) and excavation waste (*EwO*, 146 g kg^{-1}). After one year, OC increased by 23% in *CwO* and 7% in *EwO*, while remaining stable in *WCB*. However, OC decreased from year 1 to year 2 in all technosols (*WCB*: -11.8 %, *CwO*: -10.7 %, *EwO*: -4 %) (Fig. 1).

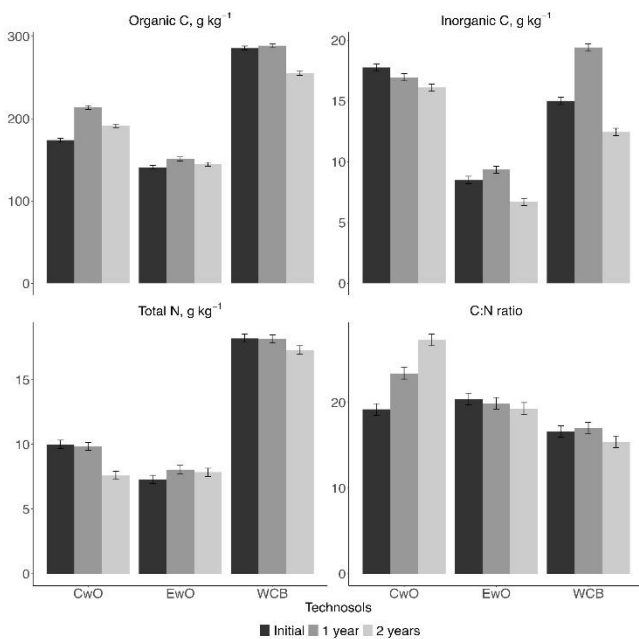


Figure 1. Total, organic and inorganic C and total nitrogen contents, and C/N ratio of technosols *CwO*, *EwO* and *WCB* over the experimental period (initial conditions, and after 1 and 2 years of experiment)

These trends suggest that despite initial variations in OC levels among technosols, the OC content remained relatively stable across all technosols in the short-term (2 years). The increase in OC content in *CwO* and *EwO* after the first year could be attributed to the occlusion of coarse and fine particulate OM within macroaggregates, which physically protects

OM and reduces its accessibility to decomposers and their enzymes (Giannetta et al. 2018). This is further supported by findings from studies on microcosms where particulate OM serves as a nucleus for effective macroaggregate formation (Bucka et al. 2019). In contrast, the significant decrease in OC from year 1 to year 2 across all technosols may be due to the loss of labile organic compounds, which are known to be more prone to decomposition, particularly when associated with macroaggregates (Nichols and Halvorson 2013; Yu et al. 2015). To maintain the stability of OC in the long term, continuous replacement or stabilization of labile compounds within aggregates is necessary (Pronk et al. 2016). Inorganic carbon (IC) levels also varied significantly among technosols ($p = 0.0154$), with *WCB* and *CwO* containing higher IC (15.6 and 16.9 g kg^{-1} , respectively) compared to *EwO* (8.2 g kg^{-1}), likely due to the presence of carbonates in *CwO* and *EwO*, as indicated by FTIR bands (Fernández-Ugalde et al. 2014). Total nitrogen (TN) contents varied among technosols ($p = 8.71e-11$) and over time ($p = 0.0020$). *WCB* had the highest TN (17.9 g kg^{-1}), followed by *CwO* (9.2 g kg^{-1}) and *EwO* (7.7 g kg^{-1}). However, TN in *CwO* decreased by 24% over two years, leading to an increase in its C/N ratio from 23 to 27, suggesting N immobilization (Nguyen et al. 2016). Additionally, as supported by data in Table 3, the presence of external mycelium (EM) and arbuscular mycorrhizal fungi (AMF) in all technosols could have played a key role in promoting N cycling. Fungi, particularly AMF, are known to enhance nutrient uptake and improve aggregate stability by enmeshing soil particles and OM (Rillig et al. 2015). This could explain the stable N contents in *EwO* and *WCB*, where microbial activity may have contributed to N retention, unlike in *CwO*, where N losses were more pronounced. C/N ratios also varied significantly ($p = 5.29e-06$) among the technosols, with *CwO* showing the highest ratio (23),

Table 3. Total amount of external mycelium (EM), arbuscular mycorrhizal fungi (AMF), mycelium of dark septate endophyte (DSE), and colonization of AMF in the rootlets collected from each Technosol. Lowercase letters compare among Technosols and mean values followed by the same letter do not differ statistically from each other according to Tukey's test at 5 % probability level.

Technosols	EM	AMF	DSE	Root colonization
	mm g ⁻¹ soil			%
CwO	3574 (689) a	1280 (562) a	2294 (467) ab	23.2 (15.0) a
EwO	2747 (689) a	1453 (562) a	1294 (467) b	21.5 (12.2) a
WCB	4640 (689) a	800 (562) a	3840 (467) a	46.2 (12.2) a

followed by *EwO* (20) and *WCB* (16). After two years, the C/N ratio in *CwO* increased by 42%, reaching 27, due to the combination of rising OC and declining TN levels. This elevated C/N ratio indicates a potential shift towards N immobilization in *CwO*, while *EwO* and *WCB* maintained stable C/N ratios under 25, favoring conditions for net N mineralization and supporting soil fertility and microbial activity. In contrast, the relatively stable C/N ratios in *EwO* and *WCB*, below 25, suggest more favorable conditions for net N mineralization, which is essential for maintaining soil fertility and microbial activity. These variations highlight the importance of understanding C/N dynamics in constructed technosols to optimize their nutrient retention and cycling capacities for long-term productivity.

Exchangeable cations in technosols

Exchangeable Ca^{2+} levels differed significantly among the technosols ($p = 0.0002$) and over the experimental period ($p = 6.94\text{e-}08$). On average, *WCB* had the highest exchangeable Ca^{2+} concentration ($62.5 \text{ cmol kg}^{-1}$), followed by *CwO* ($59.3 \text{ cmol kg}^{-1}$) and *EwO* ($54.5 \text{ cmol kg}^{-1}$). Exchangeable Ca^{2+} increased by 56%, 51%, and 35% in *EwO*, *CwO*, and *WCB*, respectively. By the end of the 2-year experiment, technosols *CwO* and *WCB* had similar Ca^{2+} concentrations (Fig. 2). The increase in Ca^{2+} is essential for promoting the formation of stable soil aggregates. The presence of polyvalent cations like Ca^{2+} can foster physicochemical associations between organic compounds and minerals, enhancing aggregate stability (Safar and Whalen 2023; Rakhsh et al. 2017). As shown in Table S4, higher concentrations of exchangeable Ca^{2+} were observed alongside the presence of mycorrhizal fungi (external mycelium and AMF), which may have contributed to the formation of stable soil aggregates through enmeshing soil particles and promoting OM turnover (Rillig et al. 2015). This is consistent with findings that link Ca^{2+} -mediated aggregation with increased soil structure stability in technosols. Exchangeable Mg^{2+} levels varied significantly among technosols ($p = 5.94\text{e-}09$) and over time ($p = 1.82\text{e-}05$). *WCB* had the highest Mg^{2+} concentrations ($17.6 \text{ cmol kg}^{-1}$), followed by *EwO* (12 cmol kg^{-1}) and *CwO* (8.8 cmol kg^{-1}). While Mg^{2+} concentrations increased across all technosols after the first year, they decreased by the second year to levels close to their initial conditions (Fig. 2). These fluctuations could be due to changes in cation exchange or leaching, impacting soil aggregate stability

and nutrient availability. Exchangeable K^+ and Na^+ concentrations showed significant differences among technosols ($p = 0.0031$ and $1.37\text{e-}10$, respectively) and over time ($p = 2.56\text{e-}08$ and $6.57\text{e-}13$, respectively). *WCB* and *CwO* had the highest K^+ concentrations (10.2 and $10.5 \text{ cmol kg}^{-1}$), compared to *EwO* ($9.44 \text{ cmol kg}^{-1}$). All technosols experienced a significant decrease in K^+ over 2 years (48%, 44%, and 18% in *EwO*, *CwO*, and *WCB*, respectively), likely due to crop uptake or leaching, which may indicate potential long-term soil fertility decline, as potassium is critical for plant functions. Exchangeable Na^+ concentrations initially were highest in *WCB* ($4.54 \text{ cmol kg}^{-1}$), followed by *EwO* ($2.57 \text{ cmol kg}^{-1}$) and *CwO* ($1.89 \text{ cmol kg}^{-1}$). Over 2 years, all technosols experienced sharp decreases in Na^+ , with reductions of 86%, 71%, and 58% in *WCB*, *EwO*, and *CwO*, respectively. By the end of the experiment, Na^+ levels in all technosols were similar, showing no significant differences (Fig. 2). The decline in Na^+ concentrations is crucial for improving soil structure, as high levels of Na^+ can lead to soil dispersion and degradation of aggregates. The washing of salts, particularly Na^+ , through the technosols would have flocculated the clay and silicate minerals, promoting aggregate formation and improving soil physical properties (Prado et al. 2020).

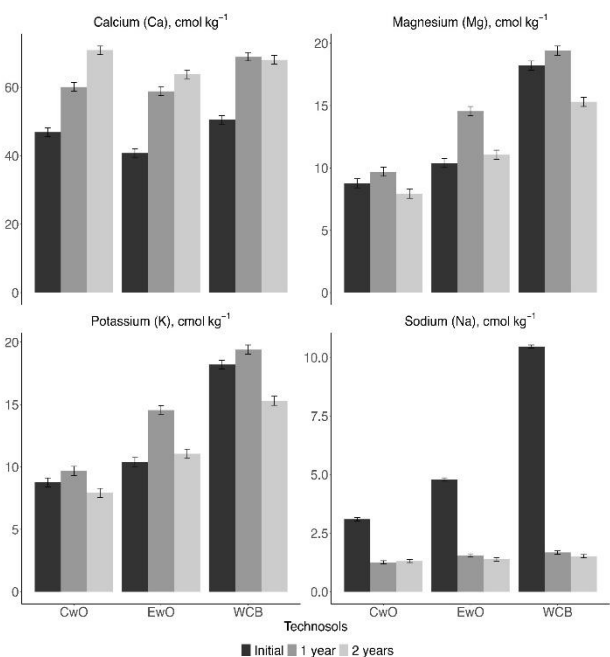


Figure 2. Concentrations of exchangeable cations (Ca^{2+} , Mg^{2+} , K^+ and Na^+) of technosols *CwO*, *EwO* and *WCB* over the experimental period (initial conditions, and after 1 and 2 years of experiment)

The reduced Na⁺ levels, combined with the increase in Ca²⁺, likely facilitated the stabilization of aggregates, enhancing the overall soil structure and C retention capacity (Safar and Whalen 2023).

Micromorphological analysis of technosols

After two years, all technosols developed sub-angular and spheroidal-granular aggregates with complex packing voids, containing both macro- and microaggregates, along with coarse and fine mineral and organic debris. *EnO* showed more sub-angular aggregates (Fig. 3), while *CwO* and *WCB* had more spheroidal-granular aggregates (Figs. 4 and 5). The occlusion of coarse and fine particulate OM within the sub-angular macroaggregates of *EnO* and *CwO* (Figs. 3 and 4) suggests that physical mechanisms may play an essential role in the protection of OC in these technosols. This occlusion likely renders OM less accessible to decomposers and microbial enzymes, contributing to C stabilization (Giannetta et al. 2018). Studies on artificial soil systems have similarly demon-

strated that particulate OM can act as a nucleus for effective macroaggregate formation (Bucka et al. 2019), and our findings corroborate the significant role of particulate OM in macroaggregate stabilization in the *EnO* and *CwO* technosols.

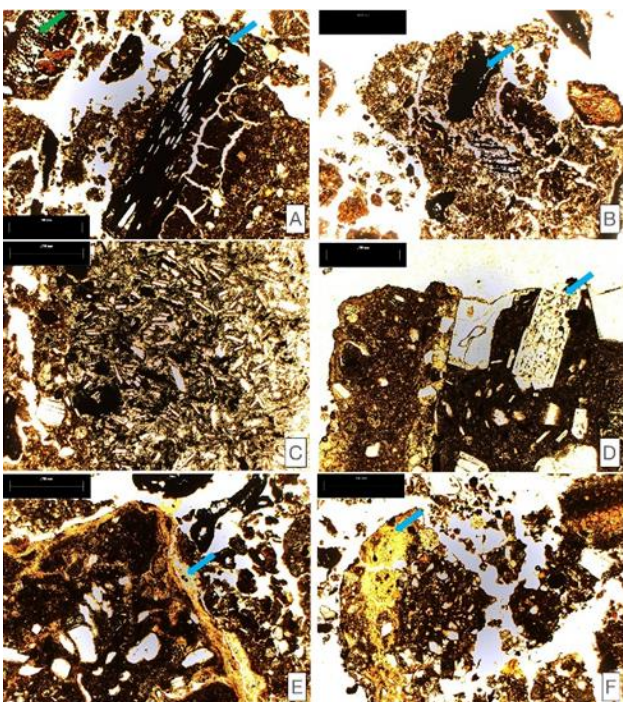


Figure 3. Micromorphological analysis of technosol *EnO*. (a) and (b) show sub-angular macroaggregates with a mixture of minerals, biochar particles (highlighted with blue arrows), plant tissue (highlighted with green arrow), and coarse organic debris within a macroaggregate. It is also possible to observe spheroidal granular microaggregates. (c) shows a basaltoid with splinters, and (d) shows carbonates and other minerals (feldspars, quartz and plagioclase) with cracks and weathering patterns. (e) and (f) show fragments of aggregates with clay illuviation (cutans)

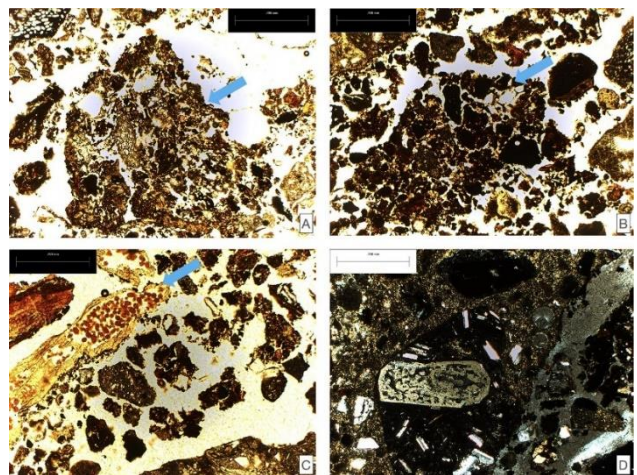


Figure 4. Micromorphological analysis of technosol *CwO*. (a) and (b) show sub-angular macroaggregates with a mixture of minerals. (c) shows a partially degraded plant tissue with mite coprolites and surrounding microaggregates. (d) with crossed Nicols shows a mixture of carbonates, basaltoids and other minerals with weathering patterns

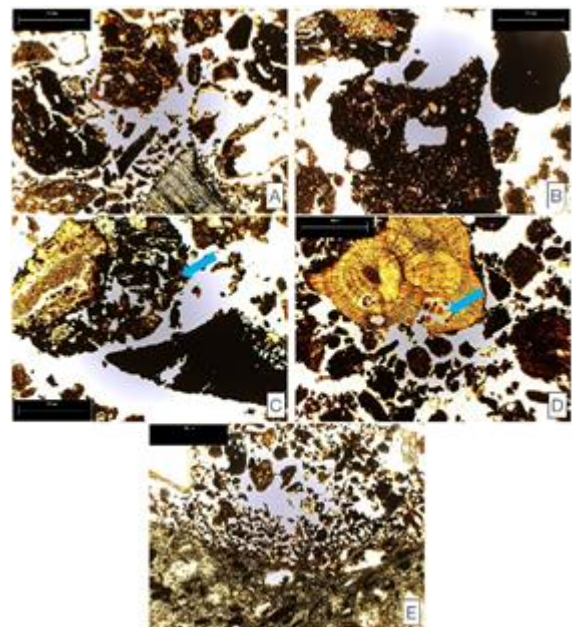


Figure 5. Micromorphological analysis of technosol *WCB*. (a) shows a biochar particle at the bottom with surrounding spheroidal microaggregates. (b) and (c) show sub-angular macroaggregates, biochar particles and carbonates. (d) shows coprolites immersed in a partially fragmented plant tissue and surrounding spheroidal microaggregates. (e) shows fragments of construction waste and spheroidal microaggregates

All technosols contained inorganic debris, including volcanic materials (basaltoids with plagioclase splinters, pumice fragments), carbonates, and other minerals (feldspars, quartz, plagioclase). Cracks and weathering patterns were observed, even in *WCB*, which had a lower inorganic content. The weathering patterns suggests that some of the minerals underwent ex-situ weathering before being used in the technosols (Fig. 3). The presence of coprolites (fecal pellets) in the *CwO* and *WCB* technosols (Figs. 4 and 5) further supports the role of soil invertebrates in enhancing soil structure. Coprolites and the activity of invertebrates like earthworms and insects contribute to aggregate formation by binding soil particles and OM. These biogenic structures may also play a significant role in the stability of aggregates in these technosols by promoting physical binding and OM turnover (Rillig et al. 2015).

Size distribution and stability of aggregates in technosols

The aggregate size distribution (Table 2) showed that large macroaggregates (> 2 mm) made up about 40%, and smaller macroaggregates (2–0.25 mm) comprised 40–50% of the total distribution in all technosols. Thus, 80–90% of the aggregates were macroaggregates. *CwO* and *WCB* had significantly more macroaggregates (8–0.25 mm) than *EnO* ($p = 0.0011$). *EnO* had more microaggregates (0.25–0.053 mm) and silt + clay particles compared to *CwO* and *WCB* ($p = 4.12e-05$ and 0.0086). Microaggregates accounted for 4–8%, with *EnO* having the highest percentage. The proportion of silt + clay particles ranged from 4% (*CwO*) to 13% (*EnO*). *WCB* had the fewest microaggregates (2%). The mean weight diameter (MWD) (2.4 mm) and geometric mean diameter (MGD) (1 mm) showed no significant differences among technosols ($p = 0.6158$ and 0.1167) (Table 3). Textural analysis revealed that both *CwO* and *EnO* were classified as sandy loam, with silt and sand-sized particles being the most abundant. *EnO* exhibited significantly higher clay content compared to *CwO* ($p = 6.99e-15$) (Table 3). Regardless of the technosol, approximately 85% of the OC, TN, and IC were found within the large (8 mm) to small (0.25 mm) macroaggregate size classes, while 5% and 10% were found in the microaggregate (0.25–0.53 mm) and silt + clay (< 0.053 mm) size classes, respectively (Fig. 6). This consistent trend highlights the critical role of macroaggregates in C and nutrient stabilization. It is well-documented that macroaggregates serve as key

repositories for OC and TN in soil systems, with occlusion of particulate OM being a primary mechanism for the stabilization of OC (Giannetta et al., 2018; Bucka et al., 2019). The occlusion of OM within macroaggregates protects it from microbial decomposition, rendering it more stable (Giannetta et al. 2018). No significant differences were observed in the distribution of OC and TN across larger aggregate size classes (8–2, 2–1, and 0.5–0.25 mm). However, *CwO* and *WCB* had significantly higher proportions of OC and TN in small macroaggregates (1–0.5 mm) compared to *EnO* ($p = 0.0020$ and $4.75e-05$). Conversely, *EnO* and *CwO* had higher proportions of OC, TN, and IC in microaggregates (0.25–0.053 mm) than *WCB* ($p = 0.0273$, 0.0291 , and 0.0377). These results suggest that smaller aggregates, like microaggregates and silt + clay particles, tend to contain more stable organic matter (Six et al. 2000; Lehmann et al. 2007). The C/N ratio of aggregates decreased from large macroaggregates (23) to silt + clay size classes (14), suggesting that smaller aggregates contain more decomposed or microbially processed OM. Significant differences were found only in small macroaggregates (0.5–0.25 mm), where *EnO* and *WCB* exhibited higher C/N ratios than *CwO* ($p = 0.0365$), indicating a higher proportion of undecomposed OM or reduced

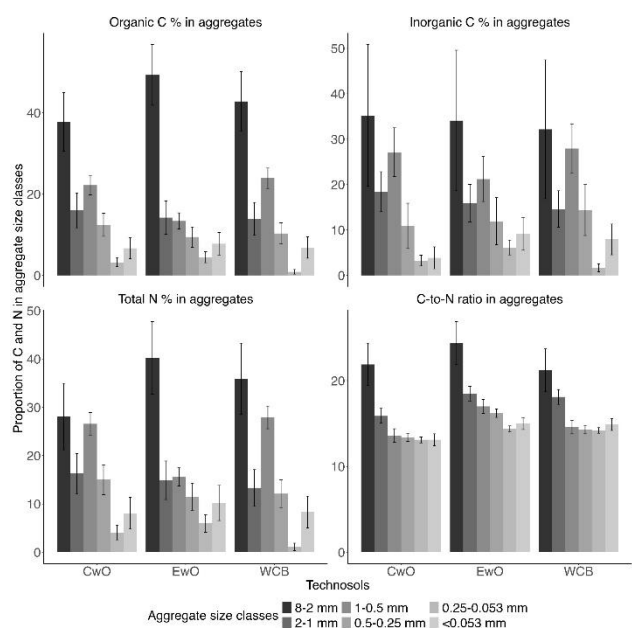


Figure 6. Organic C contents, total N content and C/N ratio of aggregate size classes of technosols produced from concrete and excavation waste combined with wood chips, compost, and biochar (*CwO* and *EnO*, respectively), and all-organic (*WCB*). Bars in grayscale represent the mean values ($n = 3$)

Table 4. Dry weight of aggregate size fractions of technosols produced from concrete and excavation waste combined with wood chips, compost, and biochar (CwO and EwO, respectively), and all-organic (WCB). Values represent the mean ($n = 3$). Lowercase letters compare technosols within each aggregate size class. Mean values followed by the same letter do not differ statistically from each other according to Tukey's test at the 5% probability level.

Technosols	Proportion of aggregate size classes (% W/W)					
	large macroaggregates	Small macroaggregates			Micro aggregates	silt + clay
	8-2	2-1	1-0.5	0.5-0.25	0.25-0.053	< 0.053
mm						
CwO	41.8 (6.05) a	17.5 (3.29) a	19.6 (1.89) ab	12.0 (2.54) a	4.08 (0.93) b	3.82 (1.54) b
EwO	36.3 (5.90) a	14.2 (3.01) a	14.6 (1.68) b	11.8 (2.52) a	8.16 (1.31) a	13.33 (2.77) a
WCB	40.2 (6.01) a	13.3 (2.93) a	24.0 (2.04) a	11.7 (2.51) a	1.98 (0.65) b	7.72 (2.16) ab

Table 5. Mean weight diameter (MWD) and mean geometric diameter (MGD) of technosols produced from concrete and excavation waste combined with wood chips, compost, and biochar (CwO and EwO, respectively), and all-organic (WCB). Values represent the mean ($n = 3$). Lowercase letters are compared among technosols and the mean values followed by the same letter do not differ statistically from each other according to Tukey's test at 5% probability level.

Technosols	MWD	MGD	Textural analysis				
			> 4 mm	4-2 mm	Sand	Silt	Clay
			mm		%		
CwO	2.57 (0.24) a	1.02 (0.01) a	136 (3.65) a	103 (14.2) a	286 (26.2) a	392 (56.4) a	83 (7.05) b
EwO	2.22 (0.24) a	0.99 (0.01) a	106 (3.28) b	99 (14.0) a	353 (27.8) a	270 (51.3) a	172 (10.2) a
WCB [†]	2.46 (0.24) a	1.01 (0.01) a	-	-	-	-	-

[†]Textural analysis was not performed in WCB due to the low presence of inorganic materials in this Technosol.

microbial activity (Nguyen et al. 2016). This distribution highlights the role of macroaggregates in protecting less decomposed OM, while smaller aggregates likely house more stabilized OM (Kögel-Knabner and Rumpel 2018).

FTIR spectra of aggregate size fractions of technosols

FTIR analysis revealed both organic and inorganic molecules essential for OM stabilization in soils. All technosols showed absorption bands for polysaccha-

rides, aliphatic and aromatic compounds, and functional groups like carbonyl, hydroxyl, and carboxylic acids (Table 6, Fig. 7), indicating the organic fraction. These compounds, mainly from organic amendments like compost, wood chips, and biochar, aid SOC stabilization through biochemical recalcitrance and mineral interactions (Liang et al. 2017). Organic macromolecules, such as lignin and cellulose, play a key role in soil structure by forming water-stable aggregates (Witzgall et al. 2021). Both EwO and CwO showed weak absorption bands for

Wave number (cm ⁻¹)	Assignment	Characterization	References
3700-3600	Hydrogen-bonded Si-O-H stretching	silicates	Russell and Fraser (1994), Madejova and Komadel (2001), Kronenberg (2018)
3300	O-H stretching	water molecules, organic compounds with hydroxyl group (alcohols, carboxylic acids, etc.)	Coates (2000), Kowalski et al. (2018)
3000 to 2800	C-H symmetric and asymmetric stretching	organic aliphatic compounds	Calderón et al. (2011), Slaný et al. (2019)
~1820	C=O stretching	organic compounds with carbonyl group (carboxylic acids, ketones, aldehydes, esters, etc.)	Lehmann et al. (2007), Calderón et al. (2013), Hernandez-Soriano et al. (2016)
~1650	C=C stretching and/or asymmetric C-O stretching	aromatic compounds	
~1450/900-875	C-O stretching	Carbonate	Nguyen et al. (1991), Russell and Fraser (1994)
1100-1000	C-O stretching and O-H deformation	polysaccharides	Artz et al. 2008

Table 6
Functional groups evaluated in the present study and their respective frequencies in mid-FTIR.

inorganic molecules, like silicates from clay minerals, indicating OM-mineral interactions, which are crucial for long-term carbon stabilization. The presence of silicates supports the role of mineral-associated OM in technosols (Safar and Whalen 2023; Rakhsh et al. 2017). Additionally, strong carbonate absorption bands were detected in *EwO* and *CwO*, aligning with their carbonate concentrations. Carbonates likely contribute to aggregate formation by enhancing stabilization mechanisms and improving soil structure through Ca²⁺-mediated cation bridges (Fernández-Ugalde et al. 2014; Safar and Whalen 2023). The presence of both organic and inorganic components in all aggregate size classes suggests that technosols have complex mechanisms for C stabilization, combining both organic compounds' recalcitrance and mineral-organic interactions (Cotrufo et al. 2019). The FTIR spectra further emphasize the importance of understanding how organic amendments and mineral particles interact to form stable aggregates and protect C in constructed soils (Kögel-Knabner and Rumpel 2018; Hoffland et al. 2020). This highlights the potential of technosols for long-term carbon storage, as these mechanisms promote both the physical protection and chemical stabilization of OM.

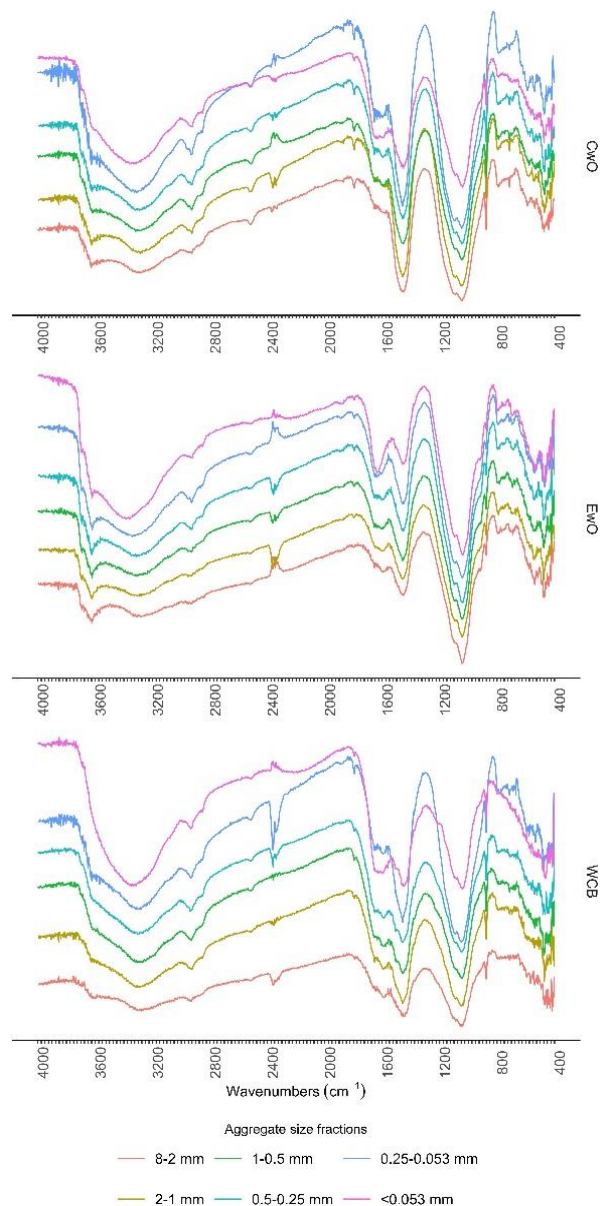


Figure 7 Fourier transform infrared (mid-FTIR) spectra of aggregate size classes of technosols produced from concrete and excavation waste combined with wood chips, compost, and biochar (*CwO* and *EwO*, respectively), and all-organic (*WCB*)

Multivariate analysis of qualitative and quantitative parameters of aggregate size classes

Principal component analysis (PCA) revealed distinct patterns among technosols, highlighting the roles of OC, IC, TN, and specific organic compounds in differentiating aggregate size classes. The first two principal components (PC1 and PC2) axes explained 77% of the variance in soil data, indicating strong differentiation among aggregate size classes and technosols (Fig. 8). PC1 explained 49% of the variance, distinguishing large and small macroaggregates from microaggregates and silt + clay fractions. High coefficients for OC, IC, TN ($r = -0.81, -0.81, -0.74$), silicates ($r = 0.65$), water ($r = 0.85$), and organic compounds like aliphatics ($r = 0.72$), carbonyls ($r = -0.68$), and aromatics ($r = 0.72$) support the hypothesis that macroaggregates contain more organic content, while finer aggregates stabilize more persistent SOC (Six et al. 2000; Lehmann et al. 2007). PC2 explained 29% of the variance, distinguishing CwO and WCB from EwO. High coefficients for polysaccharides ($r = -0.80$) and carbonates ($r = 0.60$) suggest these com-

pounds define differences between technosols. Polysaccharides, as labile organic compounds, support aggregate formation through OM decomposition and microbial activity, especially in the all-organic WCB (Bucka et al. 2019; Witzgall et al. 2021). Carbonates, more prevalent in CwO and EwO, contribute to aggregate stability via mineral-organic interactions and the formation of mineral-associated OM (Cotrufo et al. 2019; Fernández-Ugalde et al. 2014). The separation of EwO from CwO and WCB in the PCA plot highlights distinct soil properties and molecular compositions. TN in aggregates and mid-FTIR bands related to silicates, aliphatic, carbonyl, and aromatic compounds were strongly correlated with PC2 (Table 7). EwO, with higher clay content, may stabilize both labile and recalcitrant organic compounds, enhancing long-term C stabilization through organo-mineral interactions (Hoffland et al. 2020). Conversely, CwO and WCB rely more on macroaggregate formation and microbial activity for C stabilization, offering physical protection for OM, while the finer fractions in EwO may stabilize more persistent SOC (Pronk et al. 2016; Rillig et al. 2015).

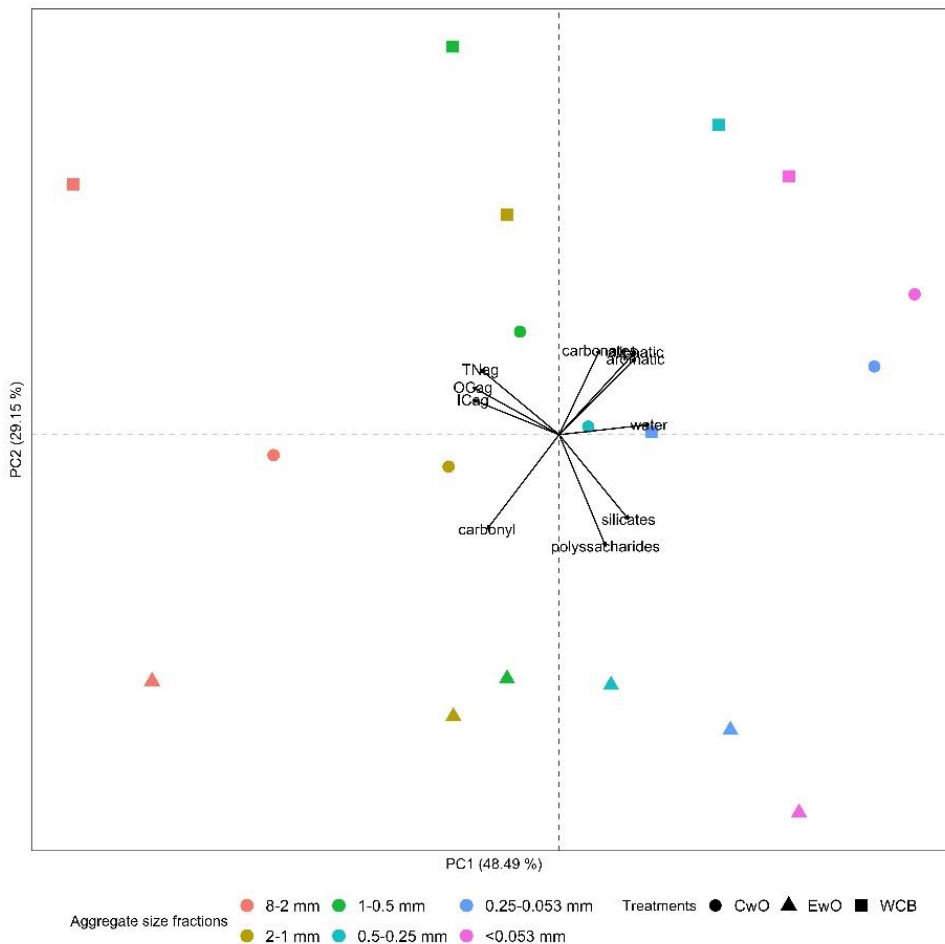


Figure 8

Principal component analysis of the chemical characterization and mid-FTIR spectra of aggregate size classes of technosols produced from concrete and excavation waste combined with wood chips, compost, and biochar (CwO and EwO, respectively), and all-organic (WCB). The segments represent each of the mid-FTIR band assignments and amounts of OC, IC and TN evaluated in aggregate size classes. OCag: Organic C in aggregates; ICag: Inorganic C in aggregates; TNag: Total nitrogen in aggregates

	PC1	PC2
Eigenvalue	4.85	2.92
Cumulative percent variation	48.49	77.64
Eigenvectors		
Organic carbon in soil aggregates (OCag)	-0.81***	0.34 ^{ns}
Inorganic carbon in soil aggregates (ICag)	-0.81***	0.25 ^{ns}
Total nitrogen in soil aggregates (TNag)	-0.74***	0.47*
3700-3600 cm ⁻¹ (O–H stretching; silicates)	0.65**	-0.61**
3300 cm ⁻¹ (O–H stretching; H ₂ O, water molecules)	0.85***	0.07 ^{ns}
3000-2800 cm ⁻¹ (C–H stretching; aliphatic)	0.72***	0.60**
1820 cm ⁻¹ (C=O stretching; carbonyl)	-0.68**	-0.68**
1650 cm ⁻¹ (C=C stretching; aromatic)	0.72***	0.55*
1450 cm ⁻¹ (C–O stretching; carbonates)	0.38 ^{ns}	0.61**
1100-1000 cm ⁻¹ (C–O stretching, O–H deformation; polysaccharides)	0.44 ^{ns}	-0.80***

Table 7

Eigenvalues, cumulative percent variation, and eigenvectors of the first two principal components (PCs) for the chemical characterization and Mid-FTIR spectra of aggregate size classes of Technosols CwO, EwO and WCB.

Overall, the multivariate analysis underscores the complex organic and inorganic interactions in technosols, with clear differences in aggregate size distribution and molecular composition affecting C and N dynamics. Further research should explore how these interactions contribute to OM stabilization across aggregate sizes, particularly in technosols (Kögel-Knabner and Rumpel 2018).

Conclusions

This study highlights the potential of technosols for OC stabilization, mainly through macroaggregation with additional contributions from microaggregation. Larger macroaggregates contained high levels of particulate OM, which protected OC from decomposition. The presence of carbonates, particularly in CwO and EwO technosols, along with increased exchangeable Ca²⁺ and decreased Na⁺, improved soil structure and aggregation through cation bridging. These interactions, particularly in CwO, facilitated OC stabilization via organomineral interactions, confirmed by the identification of silicate minerals in FTIR analysis. Such interactions suggest the formation of mineral-associated OM, essential for long-term carbon storage. Differences in C composition between macro- and microaggregates showed that recalcitrant compounds were more present in smaller aggregates,

while labile compounds were found in larger aggregates, indicating dynamic C cycling. Soil organisms, such as mycorrhizal fungi and invertebrates, further enhanced aggregate stability and organic matter turnover. Overall, technosols offer promising potential for C stabilization through physical protection and organomineral interactions. Future research should explore the role of different aggregate fractions in long-term C storage and how organic amendments and minerals can enhance technosol efficiency for C sequestration and nutrient cycling.

Acknowledgments

The authors extend their thanks to Concretos Reciclados S.A. de C.V. for providing the construction waste materials used in this investigation. They also acknowledge Ing. Alfredo Martínez Sigüenza from the Coordinación de Áreas Verdes y Forestación, Dirección General de Obras at UNAM, for the facilities provided for the installation of the experiment. Technical assistance from Dra. Maricarmen Salazar Ledesma, Biol. Jorge René Alcalá Martínez, and M.Sc. Luisa Tinoco at the Laboratorio Nacional de Geoquímica y Mineralogía (LANGEM), UNAM, is gratefully acknowledged.

Authors' contributions

All authors contributed to the study's conception, design, and analysis. Technosol experiments and sample collection were carried out by Ceres Perez Vargas and Blanca Lucía Prado Pano. Sample analysis was performed by Ceres Perez

DOI: 10.6092/issn.2281-4485/21065

Vargas, Lucy Mora Palomino, Thalita Fernanda Abbruzzini, Alan Ulises Loredo-Jasso, and María del Pilar Larrocea Ortega. Thalita Fernanda Abbruzzini led manuscript writing and data analysis, with funding from Blanca Lucia Prado Pano.

Funding

Funding for this research was provided by the DGAPA PAPIIT project (grant numbers IN102022 and IT201422).

Availability of data and material

The datasets used or analyzed during the current study are available from the corresponding author on reasonable requests.

Declarations competing interests

The authors declare that they have no known competing financial interests or personal relationships that could have appeared to influence the work reported in this paper.

References

- ABBRUZZINI T.F., REYES-ORTIGOZA A.L., ALCÁNTARA HERNÁNDEZ R.J., MORA L., FLORES L., PRADO B. (2022) Chemical, biochemical, and microbiological properties of Technosols produced from urban inorganic and organic wastes. *Journal of Soils and Sediments*, 22:146–161. <https://doi.org/10.1007/s11368-021-03062-2>
- ALMAJMAIE A., HARDIE M., ACUNA T., BIRCH C. (2017) Evaluation of methods for determining soil aggregate stability. *Soil & Tillage Research*, 167:39–45. <https://doi.org/10.1016/j.still.2016.11.003>
- BONETA A., RUFÍ-SALÍS M., ERCILLA-MONTSERRAT M., GABARRELL X., RIERADEVALL J. (2019) Agronomic and environmental assessment of a polyculture rooftop soilless urban home garden in a Mediterranean city. *Frontiers in Plant Science*, 10:341. <https://doi.org/10.3389/fpls.2019.00341>
- BUCKA F.B., KÖLBL A., UTEAU D., PETH S., KÖGEL-KNABNER I. (2019) Organic matter input determines structure development and aggregate formation in artificial soils. *Geoderma*, 354:113881. <https://doi.org/10.1016/j.geoderma.2019.113881>
- COTRUFO M.F., RANALLI M.G., HADDIX M.L., SIX J., LUGATO E. (2019) Soil carbon storage informed by particulate and mineral-associated organic matter. *Nature Geoscience*, 12:1–6. <https://doi.org/10.1038/s41561-019-0484-6>
- CRUZ-BELLO G.M., GALEANA-PIZAÑA J.M., GONZÁLEZ-ARELLANO S. (2023) Urban growth in peri-urban, rural, and urban areas: Mexico City. *Buildings and Cities*, 4:1–16. <https://doi.org/10.5334/bc.230>
- DEEB M., GRIMALDI M., LERCH T.Z., PANDO A., GIGON A., BLOUIN M. (2016) Interactions between organisms and parent materials of a constructed Technosol shape its hydrostructural properties. *Soil Discussions*, 2: 1309–1344. <https://doi.org/10.5194/soild-2-1309-2015>
- DEEB M., DESJARDINS T., PODWOJEWSKI P., PANDO A., BLOUIN M., LERCH T.Z. (2017) Interactive effects of compost, plants and earthworms on the aggregations of constructed Technosols. *Geoderma*, 305:305–313. <http://dx.doi.org/10.1016/j.geoderma.2017.06.014>
- DEEB M., GROFFMAN P.M., BLOUIN M., EGENDORF S.P., VERGNES A., VASENEV V., CAO D.L., WALSH D., MORIN T., SÉRÉ G. (2020) Constructed Technosols are key to the sustainable development of urban green infrastructure. *Soil Discussions*. <https://doi.org/10.5194/soil-2019-85>
- DÍAZ-ZORITA M., PERFECT E., GROVE J.H. (2002) Disruptive methods for assessing soil structure. *Soil & Tillage Research*, 64:3–22. [https://doi.org/10.1016/S0167-1987\(01\)00254-9](https://doi.org/10.1016/S0167-1987(01)00254-9)
- ELLERBROCK R.H., GERKE H.H. (2013) Characterization of organic matter composition of soil and flow path surfaces based on physicochemical principles: a review. *Advances in Agronomy*, 121:117–177. <https://doi.org/10.1016/B978-0-12-407685-3.00003-7>
- FERNÁNDEZ-UGALDE O., VIRTO I., BARRÉ P., APESTEGUÍA M., ENRIQUE A., IMAZ M.J., BESCANS P. (2014) Mechanisms of macroaggregate stabilisation by carbonates: implications for organic matter protection in semi-arid calcareous soils. *Soil Research*, 52:180–192. <https://doi.org/10.1071/SR13234>
- FORJÁN R., RODRÍGUEZ-VILA A., CERQUEIRA B., COVELO E.F., MARCET P., ASENSIO V. (2018) Comparative effect of compost and technosol enhanced with biochar on the fertility of a degraded soil. *Environmental Monitoring and Assessment*, 190:610. <https://doi.org/10.1007/s10661-018-6997-4>
- FROUZ J., LIVEČKOVÁ M., ALBRECHTOVÁ J., CHROŇÁKOVÁ A., CAJTHAML T., PIŽL V., HÁNĚL L., STARY J., BALDRIAN P., LHOTÁKOVÁ Z., ŠIMÁČKOVÁ H., CEPÁKOVÁ Š. (2013) Is the effect of trees on soil properties mediated by soil fauna? A case study from postmining sites. *Forest Ecology and Management*, 309:87–95. <https://doi.org/10.1016/j.foreco.2013.02.013>
- GEE G.W., OR D. (2002) Particle-size analysis. In: *Methods of Soil Analysis: Part 4 Physical Methods*, 255–293.
- GIANNETTA B., PLAZA C., VISCHETTI C., COTRUFO M.F., ZACCONE C. (2018) Distribution and thermal stability of physically and chemically protected organic matter fractions in soils across different ecosystems. *Biology and Fertility of Soils*, 54:671–681. <https://doi.org/10.1007/s00374-018-1290-9>

DOI: 10.6092/issn.2281-4485/21065

- GRARD B.J.P., CHENU C., MANOUCHEHRI N., HOUOT S., FRASCARIA-LACOSTE N., AUBRY C. (2018) Rooftop farming on urban waste provides many ecosystem services. *Agronomy for Sustainable Development*, 38:1–12. <https://doi.org/10.1007/s13593-017-0474-2>
- HERNANDEZ-SORIANO M.C., KERRÉ B., KOPITKE P.M., HOREMANS B., SMOLDERS E. (2016) Biochar affects carbon composition and stability in soil: a combined spectroscopy-microscopy study. *Scientific Reports*, 6:25127. <https://doi.org/10.1038/srep25127>
- HOFFLAND E., KUYPER T.W., COMANS R.N.J., CREAMER R.E. (2020) Eco-functionality of organic matter in soils. *Plant and Soil*, 455:1–22. <https://doi.org/10.1007/s11104-020-04651-9>
- IVASHCHENKO K., LEPORE E., VASENEV V., ANANYEVA N., DEMINA S., KHABIBULLINA F., VASENEVA I., SELEZNEVA A., DOLGIKH A., SUSHKO S., MARINARI S., DOVLETYAROVA E. (2021) Assessing soil-like materials for ecosystem services provided by constructed Technosols. *Land*, 10:1185. <https://doi.org/10.3390/land10111185>
- JANGORZO N.S., WATTEAU F., HAJOS D., SCHWARTZ C. (2015) Nondestructive monitoring of the effect of biological activity on the pedogenesis of a Technosol. *Journal of Soils and Sediments*, 1:1705–1715. <https://doi.org/10.1007/s11368-014-1008-z>
- JANGORZO N.S., WATTEAU F., SCHWARTZ C. (2018) Ranking of wetting–drying, plant, and fauna factors involved in the structure dynamics of a young constructed Technosol. *Journal of Soils and Sediments*, 18:2995–3004. <https://doi.org/10.1007/s11368-018-1968-5>
- KEMPER W.D., ROSENAU R.C. (1986) Aggregate stability and size distribution. In: KLUTE A. (Ed). *Methods of Soil Analysis, Part 1: Physical and Mineralogical Methods*. Agronomy Monograph 9, Soil Science Society of America, pp. 425–442.
- KÖGEL-KNABNER I., RUMPEL C. (2018) Advances in molecular approaches for understanding soil organic matter composition, origin, and turnover: A historical overview. In: SPARKS D.L. (Ed). *Advances in Agronomy*, Academic Press, 149:1–48. <https://doi.org/10.1016/bs.agron.2018.01.003>
- LEGUÉDOIS S., SÉRÉ G., AUCLERC A., CORTET J., HUOT M., OUVARD S., WATTEAU F., SCHWARTZ C., MOREL J.L. (2016) Modelling pedogenesis of Technosols. *Geoderma*, 262:199–212. <https://doi.org/10.1016/j.geoderma.2015.08.008>
- LEHMANN J., KINYANGI J., SOLOMON D. (2007) Organic matter stabilization in soil microaggregates: implications from spatial heterogeneity of organic carbon contents and carbon forms. *Biogeochemistry*, 85:45–57. <https://doi.org/10.1007/s10533-007-9105-3>
- LIANG C., SCHIMEL J., JASTROW J. (2017) The importance of anabolism in microbial control over soil carbon storage. *Nature Microbiology*, 2:1–6. <https://doi.org/10.1038/nmicrobiol.2017.105>
- LILAND K.H., ALMØY T., MEVIK B.-H. (2010) Optimal choice of baseline correction for multivariate calibration of spectra. *Applied Spectroscopy*, 64:1007–1016. <https://doi.org/10.1366/000370210792434350>
- LIMA G.N., FONSECA-SALAZAR M.A., CAMPO J. (2023) Urban growth and loss of green spaces in the metropolitan areas of São Paulo and Mexico City: effects of landcover changes on climate and water flow regulation. *Urban Ecosystems*, 26:1739–1752. <https://doi.org/10.1007/s11252-023-01394-0>
- LORENZ K., KANDELER E. (2006) Microbial biomass activities in urban soils in two consecutive years. *Journal of Plant Nutrition and Soil Science*, 169:799–808. <https://doi.org/10.1002/jpln.200622001>
- MAZURAK A.P. (1950) Effect of gaseous phase on water-stable synthetic aggregates. *Soil Science*, 69:135–148. <https://doi.org/10.1097/00010694-195002000-00005>
- MOREL J.L., CHENU C., LORENZ K. (2015) Ecosystem services provided by soils of urban, industrial, traffic, mining, and military areas (SUITMAs). *Journal of Soils and Sediments*, 15:1659–1666. <https://doi.org/10.1007/s11368-014-0926-0>
- MORENO-BARRIGA F., DÍAZ V., ACOSTA J.A., MUÑOZ M.A., FAZ Á., ZORNOZA R. (2017) Organic matter dynamics, soil aggregation and microbial biomass and activity in Technosols created with metalliferous mine residues, biochar and marble waste. *Geoderma*, 301:19–29. <https://doi.org/10.1016/j.geoderma.2017.04.017>
- NGUYEN T.T., CAVAGNARO T.R., NGO H.T.T., MARSCHNER P. (2016) Soil respiration, microbial biomass and nutrient availability in soil amended with high and low C/N residue – Influence of interval between residue additions. *Soil Biology and Biochemistry*, 95:189–197. <https://doi.org/10.1016/j.soilbio.2015.12.020>
- NICHOLS K., HALVORSON J.J. (2013) Roles of biology, chemistry, and physics in soil macroaggregate formation and stabilization. *Open Agriculture Journal*, 7:107–117.
- O'RIORDAN R., DAVIES J., STEVENS C., QUINTON J.N., BOYKO C. (2021) The ecosystem services of urban soils: A review. *Geoderma*, 395:115076. <https://doi.org/10.1016/j.geoderma.2021.115076>
- PRADO B., MORA L., ABBRUZZINI T., FLORES S., CRAM S., ORTEGA P., NAVARRETE A., SIEBE C. (2020) Feasibility of urban waste for constructing Technosols for plant growth. *Revista Mexicana de Ciencias Geológicas*, 37:237–249. <https://doi.org/10.22201/cgeo.20072902e.2020.3.1583>

- PRONK G.J., HEISTER K., VOGEL C., BABIN D., BACHMANN J., DING G.-C., DITTERICH F., GERZABEK M.H., GIEBLER J., HEMKEMEYER M., KANDELER E., MOUVENCHERY Y.K., MILTNER A., POLL C., SCHAUMANN G.E., SMALLA K., STEINBACH A., TANUWIDJAJA I., TEBBE C.C., WICK L.Y., WOCHER S.K., TOTSCH K.U., SCHLOTTER M., KÖGEL-KNABNER I. (2016) Interaction of minerals, organic matter, and microorganisms during biogeochemical interface formation as shown by a series of artificial soil experiments. *Biology and Fertility of Soils*, 53:9–22. <https://doi.org/10.1007/s00374-016-1161-1>
- R CORE TEAM (2021) R: A language and environment for statistical computing. R Foundation for Statistical Computing, Vienna, Austria. <https://www.R-project.org/>
- RAKSHSH F., GOLCHIN A., AL AGHA A.B., ALAMDARI P. (2017) Effects of exchangeable cations, mineralogy and clay content on the mineralization of plant residue carbon. *Geoderma*, 307:150–158. <https://doi.org/10.1016/j.geoderma.2017.07.010>
- RAPHAEL L. (2011) Application of FTIR spectroscopy to agricultural soils analysis. In: NIKOLIC G. (Ed). *Fourier Transforms — New Analytical Approaches and FTIR Strategies*. InTech, London, pp. 385–404.
- REES F., DAGOIS R., DERRIEN D., FIORELLI J.-L., WATTEAU F., MOREL J.L., SCHWARTZ C., SIMONNOT M.-O., SÉRÉ G. (2019) Storage of carbon in constructed Technosols: in situ monitoring over a decade. *Geoderma*, 337:641–648. <https://doi.org/10.1016/j.geoderma.2018.10.009>
- RILLIG M.C., AGUILAR-TRIGUEROS C.A., BERGMANN J., VERBRUGGEN E., VERESOGLOU S.D., LEHMANN A. (2015) Plant root and mycorrhizal fungal traits for understanding soil aggregation. *New Phytologist*, 205:1385–1388. <https://www.jstor.org/stable/newphytologist.205.4.1385>
- ROKIA S., SÉRÉ G., SCHWARTZ C., DEEB M., FOURNIER F., NEHLS T., DAMAS O., VIDAL-BEAUDET L. (2014) Modelling agronomic properties of Technosols constructed with urban wastes. *Waste Management*, 34:2155–2162. <https://doi.org/10.1016/j.wasman.2013.12.016>
- RUIZ F., CHERUBIN M.R., FERREIRA T.O. (2020) Soil quality assessment of constructed Technosols: Towards the validation of a promising strategy for land reclamation, waste management and the recovery of soil functions. *Journal of Environmental Management*, 276:11344. <https://doi.org/10.1016/j.jenvman.2020.111344>
- SAFAR F., WHALEN J.K. (2023) Mechanical stability of newly-formed soil macroaggregates influenced by calcium concentration and the calcium counter-anion. *Geoderma*, 430:116333. <https://doi.org/10.1016/j.geoderma.2023.116333>
- SCHMIDT H., TAYLOR P. (2014) Kon-Tiki flame cap pyrolysis for the democratization of biochar production. *Ithaca Journal*, pp. 338–348.
- SEDEMA (2021) Secretaría del Medio Ambiente del Gobierno de la Ciudad de México. *Inventario de Residuos Sólidos CDMX*. México, 160 pp.
- SÉRÉ G., SCHWARTZ C., OUVRARD S., RENAT J.-C., WATTEAU F., VILLEMEN G., MOREL J.L. (2010) Early pedogenic evolution of constructed Technosols. *Journal of Soils and Sediments*, 10:1246–1254. <https://doi.org/10.1007/s11368-010-0206-6>
- SÉRÉ G., SCHWARTZ C., OUVRARD S., SAUVAGE C., RENAT J.-C., MOREL J.L. (2008) Soil construction: a step for ecological reclamation of derelict lands. *Journal of Soils and Sediments*, 8:130–136. <https://doi.org/10.1065/jss2008.03.277>
- SIX J., ELLIOTT E.T., PAUSTIAN K. (2000) Soil macroaggregate turnover and microaggregate formation: a mechanism for C sequestration under no-tillage agriculture. *Soil Biology and Biochemistry*, 32:2099–2103. [https://doi.org/10.1016/S0038-0717\(00\)00179-6](https://doi.org/10.1016/S0038-0717(00)00179-6)
- STEVENS A., RAMIREZ-LOPEZ L. (2020) An introduction to the prospectr package. R package Vignette. R package version 0.2.1.
- TISDALL J.M., OADES J.M. (1982) Organic matter and water-stable aggregates in soils. *Journal of Soil Science*, 33:141–163. <https://doi.org/10.1111/j.1365-2389.1982.tb01755.x>
- UN-HABITAT CORE TEAM (2022) *World Cities Report 2022: Envisaging the Future of Cities*. United Nations Human Settlements Programme (UN-Habitat). Nairobi, Kenya, 387
- VERGNES A., BLOUIN M., MURATET A., LERCHN T.Z., MENDEZ-MILLAN M., ROUELLE-CASTREC M., DUBSN F. (2017) Initial conditions during Technosol implementation shape earthworms and ants diversity. *Landscape and Urban Planning*, 159:32–41. <https://doi.org/10.1016/j.landurbplan.2016.10.002>
- VIDAL-BEAUDET L., ROKIA S., NEHLS T., SCHWARTZ C. (2018) Aggregation and availability of phosphorus in a Technosol constructed from urban wastes. *Journal of Soils and Sediments*, 18:456–466. <https://doi.org/10.1007/s11368-016-1469-3>
- YU H., DING W., CHEN Z., ZHANG H., LUO J., BOLAN N. (2015) Accumulation of organic C components in soil and aggregates. *Scientific Reports*, 5:13804. <https://doi.org/10.1038/srep13804>
- WITZGALL K., VIDAL A., SCHUBERT D.I., HÖSCHEN C., SCHWEIZER S.A., BUEGGER F., POUTEAU V., CHENU C., MUELLER C.W. (2021) Particulate organic matter as a functional soil component for persistent soil organic carbon. *Nature Communications*, 12:4115. <https://doi.org/10.1038/s41467-021-24192-8>